OPEN

# Local analgesia of electroacupuncture is mediated by the recruitment of neutrophils and released β-endorphins

Jing-tao Shi[a,b], Wan-ying Cao[a], Xiao-Ning Zhang[a], Hong-Ye Wan[a], Yang-Shuai Su[a], Zheng-Yang Qu[a], Rui Wang[c], Wei He[a], Xiang-Hong Jing[a], Xiao-Yu Wang[a,*]

**Abstract**

The efficacy of acupuncture in treating pain diseases has been recognized in clinical practice, and its mechanism of action has been a hot topic in academic acupuncture research. Previous basic research on acupuncture analgesia has focused mostly on the nervous system, with few studies addressing the immune system as a potential pathway of acupuncture analgesia. In this study, we investigated the effect of electroacupuncture (EA) on the β-endorphins (β-END) content, END-containing leukocyte type and number, sympathetic neurotransmitter norepinephrine (NE), and chemokine gene expression in inflamed tissues. To induce inflammatory pain, about 200 μL of complete Frester adjuvant (CFA) was injected into the unilateral medial femoral muscle of adult Wistar rats. Electroacupuncture treatment was performed for 3 days beginning on day 4 after CFA injection, with parameters of 2/100 Hz, 2 mA, and 30 minutes per treatment. The weight-bearing experiment and enzyme-linked immunosorbent assay showed that EA treatment significantly relieved spontaneous pain-like behaviors and increased the level of β-END in inflamed tissue. Injection of anti-END antibody in inflamed tissue blocked this analgesic effect. Flow cytometry and immunofluorescence staining revealed that the EA-induced increase in β-END was derived from opioid-containing ICAM-1$^+$/CD11b$^+$ immune cells in inflamed tissue. In addition, EA treatment increased the NE content and expression of β2 adrenergic receptor (ADR-β2) in inflammatory tissues and upregulated *Cxcl1* and *Cxcl6* gene expression levels. These findings provide new evidence for the peripheral analgesic effect of acupuncture treatment by recruiting β-END–containing ICAM-1$^+$/CD11b$^+$ immune cells and increasing the β-END content at the site of inflammation.

**Keywords:** Acupuncture analgesia, Inflammatory pain, Neuroimmune, Sympathetic nerves, β-endorphin

## 1. Introduction

Acupuncture has been recognized in clinical practice to effectively relieve pain, and the therapeutic effect of acupuncture usually persists over a long period of time.[38] Numerous physiological mechanisms have been proposed to explain the pain-relieving effect of acupuncture. For example, in inflammatory muscle pain rats, low-strength electroacupuncture (EA) has been shown to reduce the introduction of pain information through the spinal gate–control mechanism, significantly alleviating pain and inhibiting the abnormal electromyography.[7] Previous studies have also demonstrated that heterotopic EA stimulation triggers the pain-inhibiting effect of diffuse noxious inhibitory controls (DNICs).[15] In addition, Han[9] found that acupuncture applied at specific frequencies to certain body sites can stimulate the release of endogenous opioid peptides in the central nervous system and activate opioid receptors to induce antinociception. Therefore, it has been deduced that acupuncture controlled pain transmission in the central nervous system by neuronal and endocrine pathways. However, the acupuncture-induced effect observed in this research was typically transient, as demonstrated by the fact that the inhibition of the C-fiber reflex caused by EA lasted 5 minutes after treatment.[44] In addition, endogenous opioid peptides are rapidly degraded by peripheral blood proteases, giving a half-life of approximately 40 minutes for β-endorphins (β-END).[42] These mechanisms could not fully explain why there is long-term pain relief after the acupuncture treatment.

During inflammation, tissue damage caused by pathogen invasion induces the release of vascular active substances and chemokines by resident tissue cells, which recruit immune cells from the blood vessels to the inflammatory site.[12] Tissue-resident and recruited immune cells secrete inflammatory mediators, including cytokines, lipid mediators, and growth factors, which activate nociceptor sensory neurons to produce pain.[26] Meanwhile, opioid-containing immune cells migrate preferentially to the

site of pain, releasing opioid peptides that activate opioid receptors on peripheral nociceptive neurons to induce antinociception.[35] Endogenous opioid peptides, including β-endorphins (β-END), enkephalins (ENK), and dynorphins (DYN), have been implicated in peripheral analgesia during the early stages of inflammation,[5] whereas antinociception is mediated only by β-END in the late stages of inflammation.[20] Owing to the presence of inflammation, opioid-producing leukocytes are progressively recruited into the pain site, resulting in the constant availability of endogenous opiopeptides and local long-term analgesic effects.

Nociceptive stimuli produced by acupuncture have been considered as one of the reasons for analgesia in previous studies.[3,43,44] Noxious stimuli can locally activate more sensory nerve fibers by axon reflexes[37]; Meanwhile, it can also locally cause symptoms such as flushing and sweating by sympathetic reflexes.[13,17] Calcitonin gene-related peptide (CGRP) released from sensory nerve fibers plays the role in vasodilation and immunosuppression. The capsaicin-induced CGRP release is sufficient to cause significant vasodilatation.[1] Calcitonin gene-related peptide can support IL-5, constrain IL-13 expression, and constrain type 2 inflammation.[24] There are also more connections between the neurotransmitter norepinephrine produced by postganglionic sympathetic nerves and immune cells. Norepinephrine can regulate $CD4^+$ T-lymphocyte and B-lymphocyte function.[11,32] Whether these 2 types of nerve fibers and their neurotransmitters can regulate local pain through the immune system is our concern.

## 2. Methods

### 2.1. Animals

Male and female Wistar rats weighing 180 to 220 g were purchased from the Institute of Laboratory Animal Science, Chinese Academy of Medical Sciences. The animals were maintained under a standard 12-hour light–dark cycle with free access to food and water. Animal experiments were reviewed and approved by the Ethics Committee of the Institute of Acupuncture and Moxibustion, China Academy of Chinese Medical Sciences (Beijing, China), and the 3 R principles were strictly followed during the experiments (project approval number: D2018-04-13-1).

### 2.2. Inflammatory pain model

Complete Freund adjuvant (Sigma-Aldrich, St. Louis, MO) was used to model chronic inflammatory pain. Rats were randomly assigned to the control group, Complete Freund adjuvant (CFA) group, EA group, anti-β-END + EA group, and 6-hydroxydopamine (6-OHDA) + EA group. Except for the control group, all rats received a 200 μL CFA injection into the left medial femoris muscle under isoflurane anesthesia. After more than 30 seconds, the needle was slowly withdrawn to prevent leakage. Animal experiments were reviewed and approved by the Ethics Committee of the Institute of Acupuncture and Moxibustion, China Academy of Chinese Medical Sciences (Beijing, China), and the 3 R principles were strictly followed during the experiments.

### 2.3. Electroacupuncture treatment

The EA treatment was applied to the region of the inflamed side with the lowest mechanical pain threshold, which was examined using a small animal algometer (SMALGO-Bioseb, Aix-En-Provenc, France). Acupuncture needles were inserted 5 mm

deep into the region and then connected to an 8-channel general-purpose stimulus generator (STG4008, Reutlingen, Germany). On the fourth day after CFA injection, EA treatment was applied for 3 days at an intensity of 2 mA and a frequency of 2 to 100 Hz for 30 minutes. The treatment was performed under isoflurane anesthesia. The rats in the control and CFA groups were treated identically without the use of EA treatment. Sterilized acupuncture needles (size 0.18 × 13 mm) were purchased from Zhongyan Taihe (Beijing, China).

### 2.4. Anti–β-endorphins serum and 6-hydroxydopamine injection

Polyclonal anti-β-END antibody was obtained from rabbit antisera and purified to a final concentration of 8 mg/mL using staphylococcal protein A-Sepharose chromatography. Thirty minutes before each EA intervention, rats in the anti-β-END + EA group were injected with 110 μL anti-β-END antibody at the site with the lowest mechanical pain threshold.

6-hydroxydopamine (Sigma-Aldrich) was dissolved in saline containing 0.2% (w/v) ascorbic acid (Sigma-Aldrich) at a concentration of 100 mg/mL. We performed local chemical sympathectomy 30 hours before the first EA intervention and 6 hours before each intervention by injecting 100 μL 6-OHDA solution into the lowest mechanical pain threshold site of 6-OHDA + EA group rats.

### 2.5. Weight-bearing experiment

To monitor changes in nonstimulus-evoked pain behavior of rats, the weight distribution of the hind paws was measured between the left (infected side) and right (control side) using a noninvasive bipedal balancer instrument. The rats were placed in a transparent plastic test box with an inclined board and forced to stand on independent pressure transducers with their hind paws. The force on both hind limbs of normal rats was balanced, but the force on the pain side of the hind limb was significantly weakened. Five independent weight readings of the ipsilateral and contralateral plates were collected from the control panel, with at least a 1-minute gap between each reading. Results were expressed as the average of the bilateral weight-bearing difference (the value of the healthy limb minus the value of the affected limb).[21]

### 2.6. Immunofluorescence/immunohistochemistry analysis

Rats were transcardially perfused with 250 mL of 0.9% saline and 250 mL of 4% paraformaldehyde solution while under deep anesthesia with 1% sodium pentobarbital solution (10 mL/kg). After perfusion fixation, tissues from the left femoral head to the ankle joint were harvested and postfixed for 24 hours before sectioning. Tissue sample randomly selected from a model group rat was embedded in paraffin and cut into 5-μm thick sections. Subsequently, the sections were stained with β-END and HE according to standard procedures.

The remaining tissues were sectioned with a cryostat (CM1950, Leica Biosystems, Wetzlar, Germany) at a thickness of 30 μm. Cryosections were blocked for 30 minutes at 37°C with 10% BSA solution containing 3% normal donkey serum and 0.5% Triton X-100 and then incubated at 4°C overnight with primary antibodies (dilution 1:500 in 0.1 M PB containing 0.5% Triton X-100). After 3 washes in 1 × PBS, the slices were incubated for 30 minutes at room temperature with a fluorescent-conjugated secondary antibody diluted 1:500 in 0.1 M PB containing 0.5% Triton X-100. The nuclei were counterstained with 4′,6-

diamidino-2-phenylindole (DAPI). The sections were visualized under a laser scanning confocal microscope (FV1200, Olympus, Tokyo, Japan), after washing with 1 × PBS. The antibodies used were a mouse monoclonal anti-β-END antibody (ab54205, Abcam, Cambridge, United Kingdom), a rabbit monoclonal anti-ICAM-1 antibody (ab206398, Abcam), a rabbit polyclonal anti-CD11b antibody (PA5-79533, Thermo Fisher Scientific, Waltham, MA), Alexa Fluor 488 Phalloidin (A12379, Life Technologies, Carlsbag, CA), donkey anti-rabbit Alexa Fluor 488 (A-21203, Thermo Fisher Scientific), and donkey anti-mouse Alexa Fluor 594 (A-21206, Thermo Fisher Scientific).

### 2.7. Enzyme-linked immunosorbent assay

Blood was collected immediately by cardiac puncture into prechilled tubes containing EDTA after EA treatment under isoflurane anaesthesia. The blood samples were allowed to clot for 2 hours at room temperature, then centrifuged at 12,000 rpm for 30 minutes at 4°C, and the supernatant serum (plasma) were collected and subsequent stored at −80°C until analysis. Rats were sacrificed with $CO_2$ asphyxiation after blood collection. The inflammatory tissues on the left side were extracted using a 12-mm skin extractor, snap frozen in liquid nitrogen and homogenized, and then transferred to 1.5 mL EP tubes. Each sample was divided into triplicate, one for total RNA extraction and the others for protein extraction. After adding the corresponding 2.5-fold mass volume of 5% acetic acid solution to the EP tube, it was heated at 100°C for 10 minutes and centrifuged at 12,000 rpm for 20 minutes at 25°C; or add the corresponding 10-fold mass volume of RIPA buffer (R0010, Solarbio, Beijing, China) containing PMSF and a protease inhibitor in the EP tube, left stand for 20 minutes at 4°C and centrifuge at 12,000 rpm for 20 minutes at 4°C. Total protein in the tissues were extracted from the supernatant and quantified using a Pierce BCA Protein assay kit (WH333439, Thermo Scientific). Finally, β-END (FEK-022-33, Phoenix Pharmaceuticals, Mannheim, Germany), CGRP (FEK-015-09, Phoenix Pharmaceuticals), IL-6 (N05059A-1, Merck Sharp & Dohme (MSD), Kenneworth, NJ), and NE (BAE-5200R, LDN, Nordhorn, Germany) were detected in the extracted proteins according to the manufacturer's instructions.

### 2.8. Flow cytometry

Rats were anesthetized with isoflurane, and left popliteal lymph node and surrounding inflammatory tissue were dissected and processed to prepare cell suspensions according to the manufacturer's instructions (130-098-305, Miltenyi Biotec, North Rhine-Westphalen, Germany). After digesting the tissue with gentleMACS, the cell suspensions were filtered into 15 mL centrifuge tubes through 70 μm nylon strainers (352350, FALCON, Tewksbury, MA). Strainers were gently rinsed with 5 mL 1 × PBS to obtain a single-cell suspension, followed by centrifugation at 300*g* for 10 minutes at 4°C, and the supernatant were discarded. Cells were washed 2 times with 5 mL 1 × PBS (containing 1% FBS) by using continuous steps of resuspension, centrifugation at 300*g* for 5 minutes at 4°C, and supernatants discarded. After fixation and permeabilization, respectively, at room temperature according to the kit instruction (ab185917, Abcam), these cells were incubated in the dark with the following antibodies: anti-β-END antibodies conjugated with APC (ab201807, Abcam), PE Mouse anti-Rat CD11b (562105, BD Pharmingen, New Jersey), and anti-ICAM1 antibodies conjugated with CY405 (ab201798, Abcam). After incubation, cells were washed 2 times with 1X PBS (containing 1% FBS), gently

resuspended in 2 mL 1 × PBS, and transferred to flow tubes. Flow cytometry was used to analyze cells after incubation (FACS Celesta, BD Bioscience). The data were then analyzed further using the FlowJo software (Tree Star).

### 2.9. Western blot analysis

Total proteins were isolated from tissue samples in each group using RIPA buffer for Western blot (WB) assays. The extracted proteins (40 μg per sample as determined by the BCA protein assay) were subjected to 90 minutes of sodium dodecyl sulfate–12% polyacrylamide gel electrophoresis (SDS-PAGE) with β-actin as an internal reference (YM3028, Immunoway). The proteins were then transferred to polyvinylidene difluoride (PVDF) membranes and blocked for 2 hours with 5% nonfat milk in TBST. Monoclonal antibodies against ADR-β2 (dilution 1:5000 in 5% nonfat milk-TBST, Abcam) were added onto the membranes and incubated at room temperature for 10 minutes, then overnight at 4°C. After washing with TBST, the membranes were incubated for 40 minutes at room temperature with 1:2000 HRP-conjugated secondary antibody–labeled IgG antibody diluted in 5% nonfat milk-TBST. Enhanced chemiluminescence (ECL) detection reagent (Amersham Pharmacia Biotech, Amersham, United Kingdom) was added to the membranes for 3 minutes, and the images were exposed to radiographic film. Finally, film autoradiograms were analyzed and quantified using the Quantity One 4. 60 software.

### 2.10. RNA-sequencing

RNA-sequencing (RNA-seq) analysis was performed by Allwegene Technology Inc, Beijing, China. Total RNA was extracted from the inflamed tissue samples of the control group, CFA group, and EA group, and its concentration, purity, and integrity were determined. The length of the RNA fragment was detected using the Agilent 2100 bioanalyzer instrument (Agilent). Then, a cDNA library is constructed by PCR amplification. After quality control, clean read pairs were obtained using the Illumina second-generation high-throughput sequencing platform with the PE150 sequencing strategy. Complete comparison and transcript splicing analysis was performed using star and Cufflinks software and then quantitative analysis on all genes. Gene expression levels were measured using the HTSeq software and quantified as the ratio of reads mapped to a gene to the gene length in kbp and expressed as the fragments per kb of transcript per million fragments mapped (FPKM).

### 2.11. Quantitative real-time polymerase chain reaction

To validate the transcriptome sequencing data, we used real-time PCR to determine the mRNA levels of 3 individual genes implicated in chemotaxis. The first-strand cDNA was synthesized using 2 μg total RNA and PrimeScript RT Master Mix (Takara, Japan). cDNA of *Cxcl1*, *Ccl5*, and *Cxcl6* were amplified. Quantitative real-time PCR amplification was performed using the ABI 7500 Real-Time PCR Systems (Applied Biosystems). The amplification procedure was as follows: one cycle of 30 seconds at 95°C for predegeneration followed by 40 PCR cycles of 5 seconds at 95°C and 40 seconds at 60°C. The primers used were as follows: Ccl5 forward 5′-CCTCACCGTCATCCTCGTT-3′ and reverse 5′- GACTG-CAAGGTTGGAGCACT-3′, Cxcl1 forward 5′- GCACCCAAACC-GAAGTCAT-3′ and reverse 5′- GGGGACACCCTTTAGCATCT-

3′, and Cxcl6 forward 5′- CCCCAAGGTGGAAGTCATAG-3′ and reverse 5′- GTGCATTCCGCTTTGTTTTC-3′. The Ct values of the target genes and the reference gene were obtained from the amplification curve. Three replicates were performed for each sample, and the relative quantification of gene expression was calculated using the $2^{-\Delta\Delta Ct}$ method.

### 2.12. Statistical analysis

All data were presented as means ± SEM. To compare variables between groups, 1-way analysis of variance was used followed by the Tukey HSD test where appropriate. *#&$P <$ 0.05 or **$P <$ 0.01 was considered statistically significant. Statistical analysis was performed using SPSS software 21.0. Pearson correlation analysis was used to determine correlations.

## 3. Results

### 3.1. Electroacupuncture treatment alleviate inflammatory muscle pain by increasing the content of β-endorphins in inflammatory tissue

We collected the 15 days data of 8 groups that received CFA injection given by intramuscular injection in medial femoris muscle (**Fig. 1A**). We used weight-bearing as an index of nonstimulus-evoked nociception (**Fig. 1B**). Intramuscular injection of CFA resulted in persistent pain and inflammation. After injection of CFA, the difference
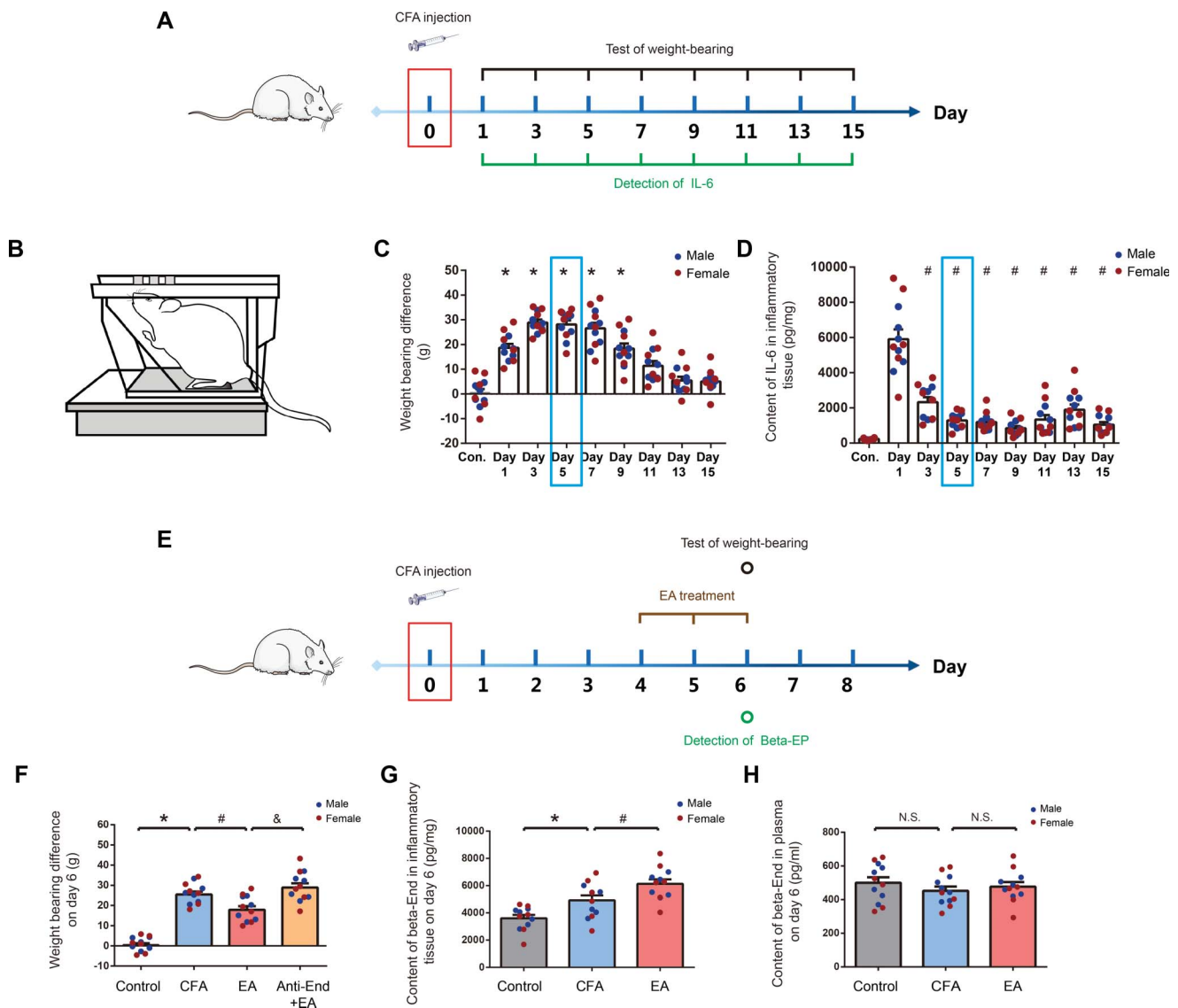


**Figure 1.** EA treatment increased the content of β-END in inflammatory tissues and relieved pain. (A) Experimental procedure timeline of observation of pain and local inflammatory reaction after intramuscular injection of CFA. N = 6 male and 6 female Wistar rats per group, total of 9 groups: control, day 1, day 3, day5, day 7, day 9, day 11, day 13, and day15. Injections were given intramuscularly. (B) A schematic illustration of behavioral testing. Changes in weight-bearing difference (C) and Interleukin- 6 (IL-6) levels in inflammatory tissues (D) measured at 15 days after CFA injection, *$P <$ 0.05 vs control group, #$P <$ 0.05 vs day 1. (E) Experimental procedure timeline of EA treatment. N = 6 male and 6 female Wistar rats per group, total of 4 groups: control, CFA, EA, and Anti-End + EA (antibody concentration: 8 mg/mL, 110 μL). (F) Weight-bearing difference was tested on day 6 after CFA injection in the indicated groups, *$P <$ 0.05 vs control group, #$P <$ 0.05 vs CFA group, &$P <$ 0.05 vs EA group. β-END levels in the tissues (G) and plasma (H) were measured on day 6 after CFA injection and EA treatment, *$P <$ 0.05 vs control group, #$P <$ 0.05 vs CFA group. All data are shown as mean ± SEM; statistical analyses were performed using one-way ANOVA followed by the Tukey honestly significant difference (Tukey HSD) test. ANOVA, analysis of variance; β-END, β-endorphins; CFA, complete Frester adjuvant; EA, electroacupuncture.

in weight-bearing and the content of IL-6 in inflammatory tissue were significantly increased. Day 4 to 6 after CFA injection was chosen for EA treatment because of the relative stationary pain and inflammatory response (blue box showed in **Figs. 1C and D**). Considering sexual dimorphism in pain reaction, we compared the weight-bearing difference and IL-6 levels in inflammatory tissues between genders in these groups. Yet, we did not observe obvious gender differences (Fig. S1A and S1B, available as supplemental digital content at http://links.lww.com/PAIN/B798). On day 6 after the injection, weight-bearing differences between 4 groups of rats were determined, as shown in **Figure 1F**. After EA treatment, the difference in weight-bearing in rats was significantly reduced when compared with the CFA group. In addition , a local injection of the anti-End antibody neutralized the analgesic effect, as indicated by an increase in the weight-bearing difference in the anti-End + EA group. As shown in **Figure 1G**, the β-END content in inflammatory tissue was significantly increased in the CFA group as compared with the control group. After EA treatment, the levels of β-END in inflammatory tissue were significantly increased compared with the CFA group. However, there were no significant differences in the β-END content of peripheral blood between the control, CFA, and EA groups (**Fig. 1H**). We compared the analgesic effects of EA between genders in these 4 groups and did not observe obvious gender differences in the analgesic effects (Fig. S2A, S2B and S2C, available as supplemental digital content at http://links.lww.com/PAIN/B798).

### 3.2. Increased numbers of β-endorphins containing ICAM-1+/CD11b+ immune cells in inflammatory tissue were associated with electroacupuncture treatment

After CFA injection, obvious inflammatory reaction occurred in muscle tissue of the injection site (**Fig. 2A**). Inflammatory cell infiltration was observed in paraffin section with immunohistochemical staining of β-END. The presence of β-END positive cells was observed both in localized inflammation and draining lymph node. Based on the morphology of the nuclei, we speculated that β-END–positive cells were neutrophils, macrophages, and monocytes (**Fig. 2B**). In frozen section with immunofluorescence staining, confocal microscopy was performed to assess colocalization of β-END and ICAM-1 or CD11b, which were common markers of neutrophils, monocytes, and macrophages. The results showed that EA treatment led to increase the number of opioid-containing ICAM-1+/CD11b+ cells in the inflammatory tissues (**Figs. 2C and D**).

### 3.3. Electroacupuncture induces the release of β-endorphins from immune cells of ICAM-1+/CD11b+ in inflammatory tissues

In the early phase after CFA injection, innate immune cells in the blood circulation and local connective tissue were mobilized, resulting in the recruitment of granulocytes and monocytes in inflammatory tissue. Flow cytometry was used to measure the percentage of granulocytes (GRAs) and monocytes (MONs) in draining lymph nodes and inflammatory tissue on day 6 after CFA injection (**Fig. 3A**). The proportions of GRAs and MONs in the EA group were significantly higher than those in the CFA group and much higher than those in the control group (**Fig. 3B**). Simultaneously, the proportions of β-END+ GRAs and MONs were significantly lower in the EA group than in the CFA group, and much lower than the control group (**Figs. 3C and D**). Compared with the CFA group, EA treatment significantly reduced the proportions of β-END and CD11b coexpression in GRAs and MONs (**Figs. 3F and G**). Meanwhile, the proportions of β-END and ICAM-1 coexpression in GRAs and MONs were also reduced in the EA group (**Figs. 3H and I**). The findings suggested that the EA induced the release of β- END from immune cells of ICAM-1+/CD11b+ in inflammatory tissues.
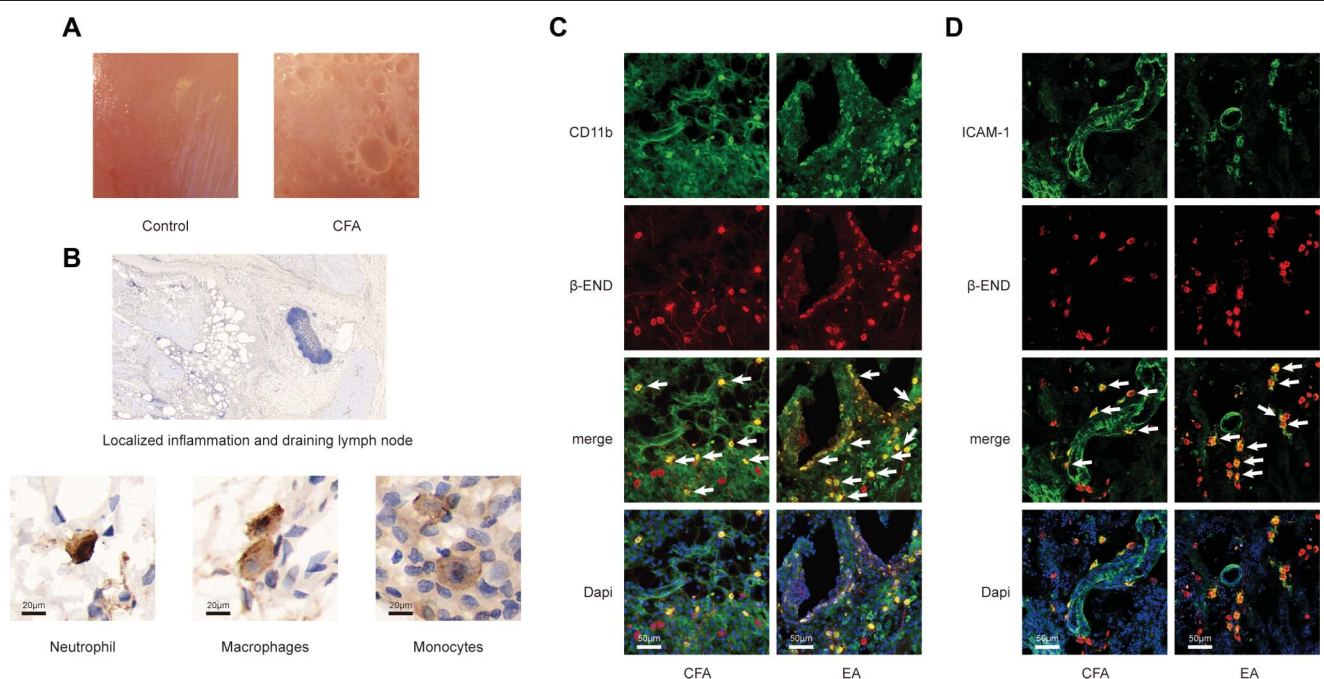


**Figure 2.** EA treatment increased the number of β-END containing ICAM-1+/CD11b+ immune cells in inflammatory tissue. (A) Representative examples of muscles from rats after CFA injection and control treatment. (B) Immunohistochemistry images of sections stained with β-END showing inflammatory cell infiltration. Dark brown staining represents β-END immunoreactivity. Neutrophils exhibited a typical polymorphic nucleus, macrophages exhibited an elongated or indented oval nucleus, and monocytes exhibited an oval notched or horseshoe-shaped nucleus. (C and D) Immunofluorescence staining of inflammatory tissue using a mouse anti-β-END antibody (red), rabbit anti-ICAM-1 antibody or anti-CD11b antibody (all were marked green), and DAPI. Arrows point at double-positive cells. β-END, β-endorphins; CFA, complete Frester adjuvant; EA, electroacupuncture.
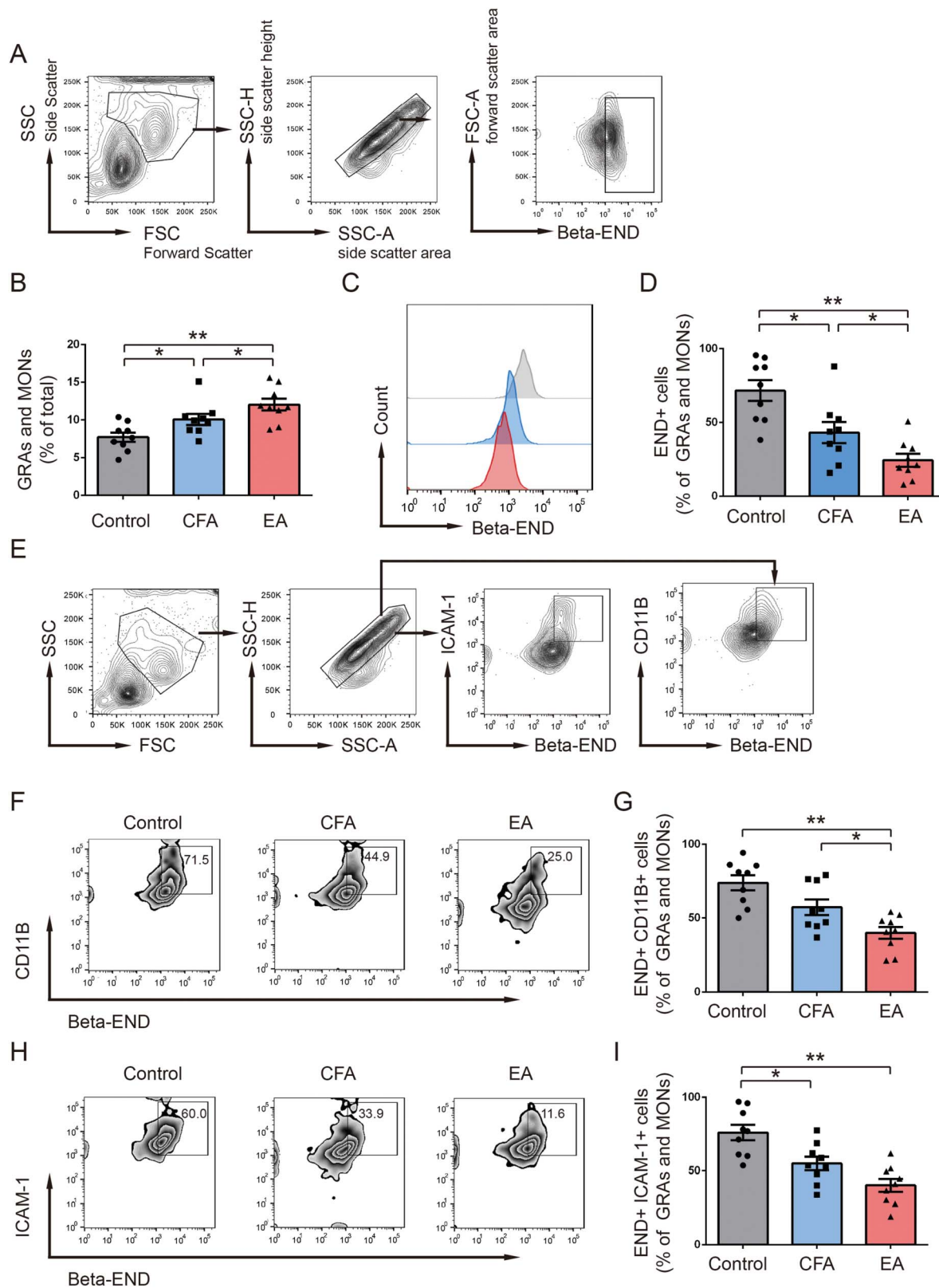
**Figure 3.** EA treatment increased proportions of GRAs and MONs and decreased the proportions of β-END⁺ CD11b⁺ and β-END⁺ ICAM-1⁺ cells on day 6 after CFA injection. (A) Flow cytometry plots showed the gating strategy for β-END⁺ cells in GRAs and MONs. (B) Bar graph showed the change of GRAs and MONs (% of total) on day 6 after CFA injection in 3 groups (n = 9). (C and D) Flow cytometry plots and bar graph show the expression of β-END in GRAs and MONs in 3 groups (n = 9). (E) Gating strategy of β-END⁺ ICAM-1⁺ cells and β-END⁺ CD11b⁺ cells in GRAs and MONs. Flow cytometry plots and bar graphs show the proportions of β-END⁺ CD11b⁺ (F and G) and β-END⁺ ICAM-1⁺ (H and I) cells in GRAs and MONs in 3 groups. **$P < 0.01$ vs control group, #$P < 0.05$ vs CFA group. All data are shown as mean ± SEM; statistical analyses were performed using 1-way ANOVA followed by the Tukey HSD test. ANOVA, analysis of variance; β-END, β-endorphins; CFA, complete Frester adjuvant; EA, electroacupuncture; FSC, forward scatter; FSC-A, forward scatter area; GRAs, granulocytes; MONs, monocytes; SSC, side scatter; SSC-A, side scatter area; SSC-H, side scatter height.

### 3.4. The sympathetic nerve is associated with the analgesic effect of electroacupuncture treatment

On day 6 after CFA injection, CGRP released by sensory nerve fibers and *Crcp* (CGRP receptor component) gene expression in inflammatory tissue was significantly increased in the CFA group. However, no significant difference in CGRP contents or *Crcp* gene expression was observed between the CFA and EA groups (**Figs. 4A and B**). Meanwhile, CFA injection led to a decrease in NE release from sympathetic nerves, whereas EA treatment increased the NE content and expression of β2 adrenergic receptor (ADR-β2) in inflammatory tissues (**Figs. 4C and F**). To elucidate the role of the sympathetic nerve in this process, we used chemical sympathectomy by local intramuscular injection of 6-OHDA. After sympathetic ablation, there was a drastic

reduction of NE content in the 6-OHDA + EA group (**Fig. 4C**). The local injection of 6-OHDA neutralized the analgesic effect of EA treatment, as indicated by the increase in the weight-bearing difference in the 6-OHDA + EA group (**Fig. 4D**).

### 3.5. RNA-sequencing analysis and validation of quantitative real-time PCR

To further investigate the effect of EA on the migration of opioid-containing cells, we used RNA-seq to perform transcriptomic analysis of inflammatory tissues. As shown in **Figure 5A**, the mRNA levels of cell migration–associated genes obtained from RNA-seq were plotted as a heat map. Differentially expressed genes between the CFA and EA groups were selected and
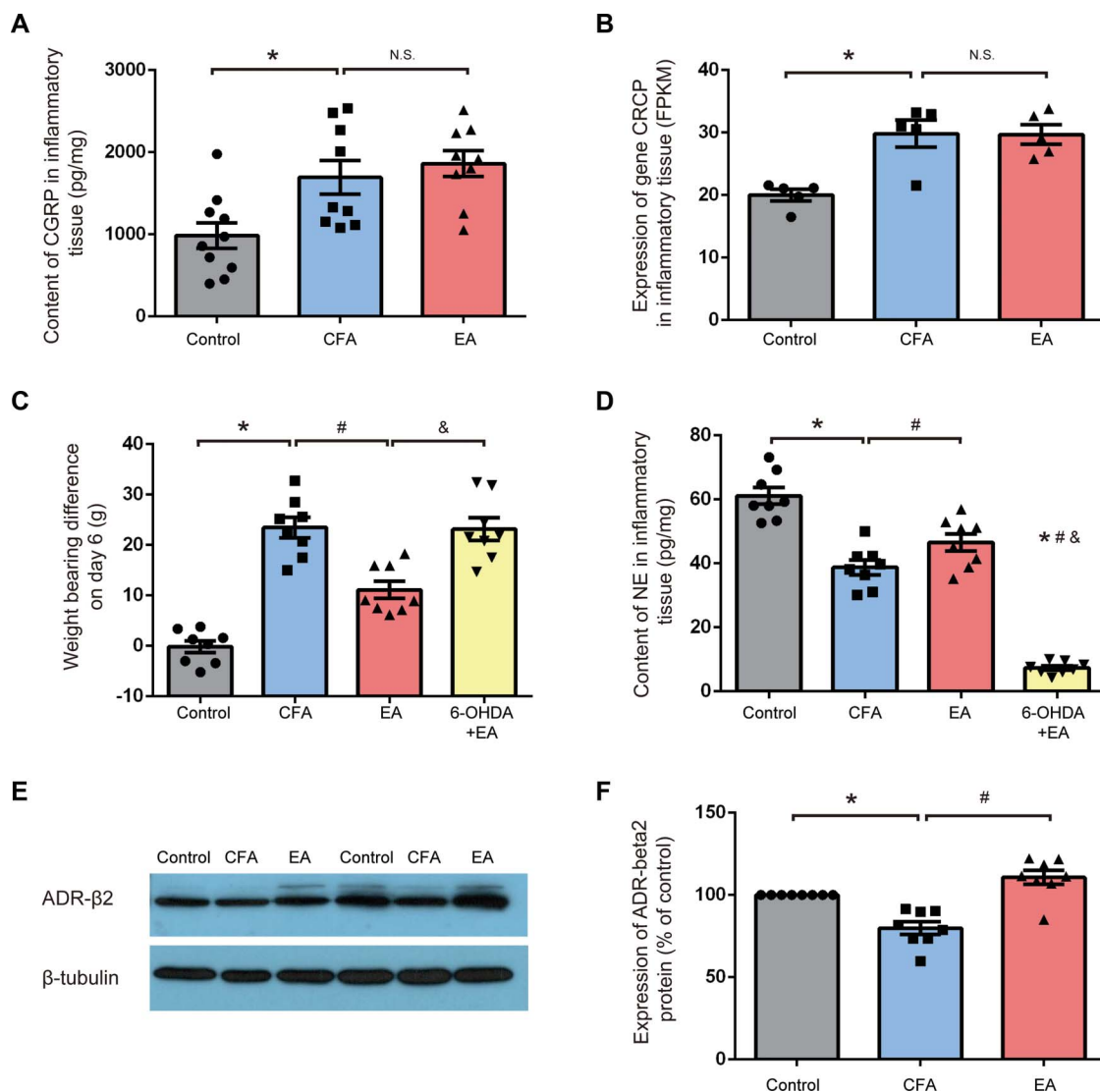


**Figure 4.** Sympathetic nerve mediating the analgesic effect of EA treatment. (A) Compared with the control group, content of CGRP in inflammatory tissue was higher in the CFA group, but it was not significantly different between the CFA group and EA group (n = 9). (B) Expression of gene *Crcp* in FPKM was generated from whole-transcriptome sequencing in result 5. Compared with the control group, expression of gene *Crcp* in inflammatory tissue was higher in the CFA group, but it was not significantly different between the CFA group and EA group (n = 5). (C) Contents of NE was measured on day 6 after CFA injection in the control, CFA, EA, and 6-OHDA + EA groups (n = 8). *$P < 0.05$ vs control group, #$P < 0.05$ vs CFA group, &$P < 0.05$ vs EA group. (D) Weight-bearing difference was tested on day 6 after CFA injection in the control, CFA, EA, and 6-OHDA + EA groups (n = 8). *$P < 0.05$ vs control group, #$P < 0.05$ vs CFA group, &$P < 0.05$ vs EA group. (E) Expression of β2 adrenergic receptor as determined by the Western blotting test. (F) Compared with the control group, ADR-β2 expression in inflammatory tissue was lower in the CFA group. ADR-β2 expression in the EA group was significantly higher compared with the CFA group (n = 8). *$P < 0.05$ vs control group, #$P < 0.05$ vs CFA group. All data are shown as mean ± SEM; statistical analyses were performed using 1-way ANOVA followed by the Tukey HSD test. ADR-β2, β2 adrenergic receptor; ANOVA, analysis of variance; CFA, complete Frester adjuvant; CGRP, calcitonin gene-related peptide; EA, electroacupuncture; FPKM, fragments per kb of transcript per million fragments mapped; NE, norepinephrine; OHDA, hydroxydopamine.

drawn as Violin plots. As shown in **Figure 5B**, EA treatment significantly upregulated *Cxcl1* and *Cxcl6* gene expression levels and downregulated *Ccl5* gene expression levels when compared with the CFA group. Although there was no statistically significant difference in Icam1 gene expression between the CFA and EA groups, there was a tendency toward significance. The expression levels of the chemokine genes were then validated using quantitative real-time PCR. The variations in genes expression were consistent with the RNA-seq analysis results (**Fig. 5C**). To demonstrate the correlation between sympathetic nerves and chemokine genes, we analyzed the correlation between the NE content and *Cxcl1* gene expression in inflammatory tissues. Pearson correlation coefficient analysis revealed a positive correlation, $r = 0.5080$, $P = 0.0445$(**Fig. 5D**).

## 4. Discussion

The major finding of this study is that EA exerts a local analgesic effect during peripheral inflammation by activating sympathetic nerve fibers and promoting the migration of β-END containing ICAM-1$^+$/CD11b$^+$ immune cells to the pain site. This is demonstrated by the following findings: (1) EA treatment significantly alleviated spontaneous pain behavior in rats by increasing the amount of β-END in local inflammatory tissue, whereas local subcutaneous administration of an anti-End antibody blocked this analgesia; (2) EA treatment significantly increased the number of β-END containing ICAM-1$^+$/CD11b$^+$ immune cells in inflammatory tissues; (3) EA treatment significantly decreased the proportion of cells with β-END co-expressed with ICAM-1 or CD11B in granulocytes and monocytes; (4) finally, EA upregulated the expression levels of NE and
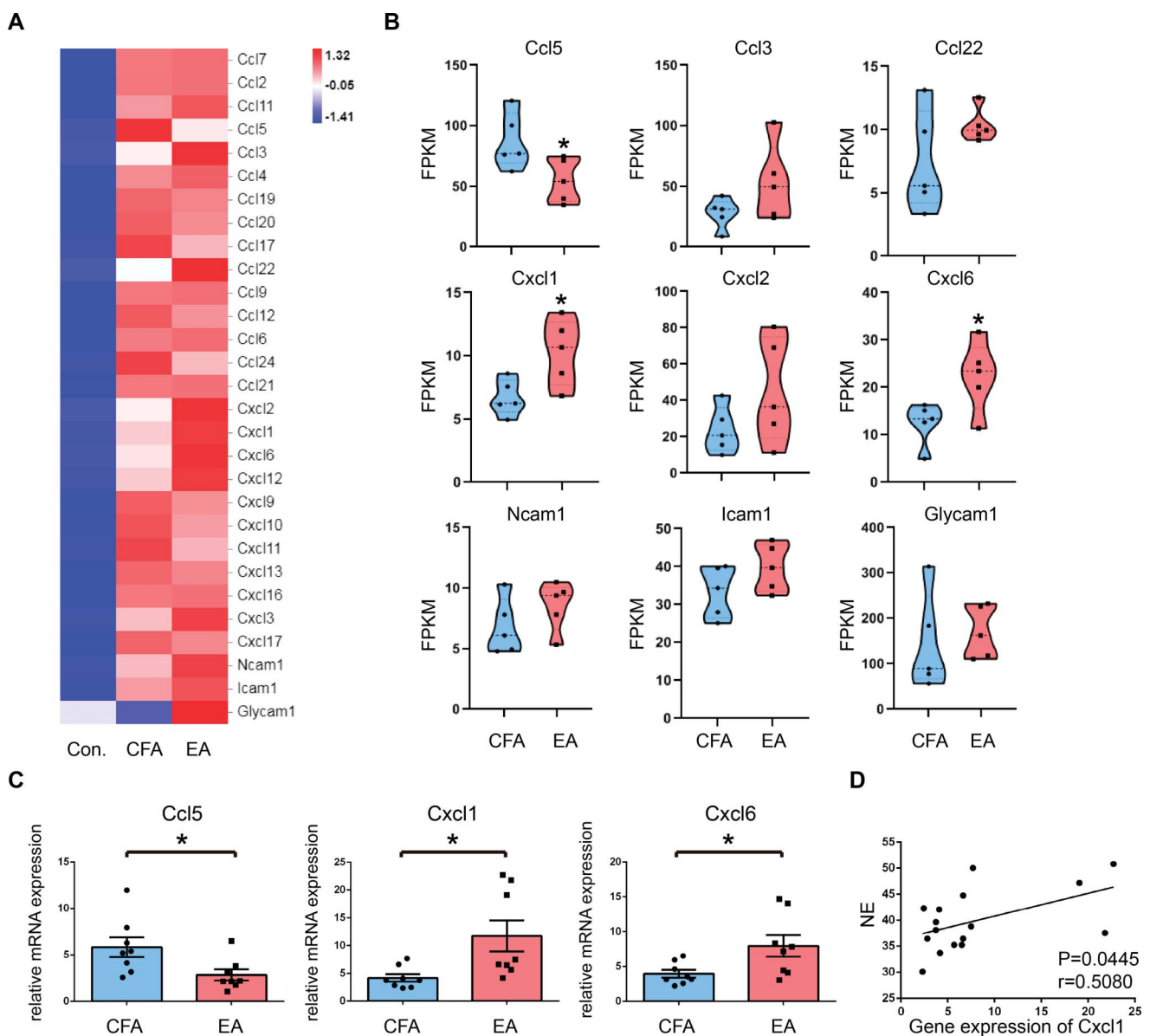


**Figure 5.** RNA-sequencing analysis and qRT-PCR verification of genes related to cell migration. (A) Heat map of cell migration–associated genes. Different heat map colors represent the relative mRNA expression levels of genes calculated by Log$_2$ (FPKM + 1). (B) Violin plots of expression values for differentially expressed genes between CFA and EA groups. Results are expressed as FPKM. Data shown are the mean FPKM ± SEM (n = 5). *$P < 0.05$ vs CFA group. (C) Significant differentially expressed genes as determined by real-time PCR (n = 8). (D) Correlation between NE and the gene expression of *Cxcl1* in inflammatory tissues based on the Pearson correlation analysis. All data are expressed as the mean ± SEM. *$P < 0.05$ vs CFA group. CFA, complete Frester adjuvant; EA, electroacupuncture; FPKM, fragments per kb of transcript per million fragments mapped; NE, norepinephrine.

β2-ADR in inflamed tissue, and 6-OHDA treatment completely offset the analgesic effect of EA.

In the present and previous studies, the nervous system is often the target of acupuncture analgesia mechanisms. Acupuncture has been shown to suppress or block the introduction of damaging sensory impulses in different levels of the central nervous system, including the spinal dorsal angle and PAG, thus exerting an analgesic effect.[43] However, few studies have examined the immune system as a potential pathway for pain control with acupuncture treatment. Numerous studies in the field of pain have found that immune cells containing opioids preferentially migrate to the injured tissues, releasing opiopeptides, and activating the opioid receptors on peripheral sensory nerve terminals, thereby inhibiting inflammatory pain.[10] Researchers discovered that both central and peripheral opioid peptides were implicated in the antinociceptive effect of early inflammation by activating the corresponding receptors. Antinociception was primarily induced at a later stage of inflammation by the interaction between leukocyte-derived β-END and peripheral opioid receptors.[20] In this study, local injection of β-END–neutralizing antibodies counteracted the analgesic effect of acupuncture analgesia, indicating that acupuncture may mediate analgesia by increasing β-END levels in peripheral tissues.

Selectors mediate opioid-containing immune cells in normal tissues by rolling close to vessel walls, trafficking between the blood and lymphatic systems, and very rarely into the tissue. When inflammation occurs, the cells activated by inflammatory media and chemokines adhere to the vascular wall of the inflammatory site, exiting the circulation and extravasating to inflammatory foci.[14] The binding of ICAM-1 to leukocyte β2 integrin is essential for leukocyte transendothelial migration.[41] Blockade of β2 integrins or ICAM-1 by monoclonal antibodies significantly decreased the infiltration of leukocytes expressed opioid peptides in inflamed tissue and abolished stress-induced peripheral antinociception.[18,19] Mac-1 (CD11b/CD18) plays a role in the adhesion of stimulated neutrophils to the vascular endothelium during CFA-induced local inflammation.[6,30] According to previous studies, the peripheral endogenous opioid peptides that mediate the local antinociceptive effect are mainly derived from monocytes or macrophages during the late stages of inflammation.[4,28] Acupuncture was shown to achieve

endogenous pain control by increasing the expression of chemokine CXCL10 and the number of infiltrating CXCR3^{+} macrophages expressing opiopeptides.[40] We now extend these findings by demonstrating that EA treatment selectively targeted opioid-containing ICAM-1^{+}/CD11b^{+} cells to the pain site and increased local tissue content of β-END. However, the non-specific nature of ICAM-1 and CD11B makes it difficult to distinguish between leukocyte types that produce β-END.

In this study, we found that the activation of the sympathetic nerve was involved in the local analgesic effect mediated by EA, and chemical sympathectomy completely abolished intrinsic opioid analgesia. The sympathetic nervous system stimulated adrenergic receptors on inflammatory cells by producing NE and releasing β-END into peripheral inflamed tissue.[2] In addition, the NE secreted by sympathetic nerves regulates immunological response primarily by β2-adrenergic receptors (β2-AR) expressed on lymphocytes.[34] Although most studies suggest that β2-AR agonists have immuno-suppressive effects, numbers studies suggest that β2-AR activation on immune cells can enhance inflammation by MAPK signaling pathways.[16] The enhanced expression of endothelial cell ICAM-1 and the subcutaneous recruitment of opioid peptide–containing neutrophils and monocytes during painful paw inflammation have been demonstrated to be caused by sympathetic fibers.[22] The use of β-blocker decreases the expression of chemokine receptor 2 (CCR2) and peripheral blood leukocytes infiltration into the site of damage.[8] By acting on β-ARs expressed on nonhematopoietic cells, the sympathetic nerve has been demonstrated to generate circadian changes in the expression of endothelial cell adhesion molecules and chemokines and to regulate rhythmic recruitment of leukocytes to the inflammatory site.[33] Some researchers have observed that the activation of β2-AR inhibited antigen-primed T cells egress from LNs by interactions with CCR7 and CXCR4.[25] The effect of SNS on cell migration may provide insight into the endogenous opioid analgesic mechanism induced by EA.

After that, we evaluated the effect of EA on the expression of chemokine genes, which play an important role in the regulation of leukocytes migration and the perception of pain.[36] Cxcl1 and Cxcl6 have been shown to act as specific chemoattractants for polymorphonuclear neutrophils.[27] In addition, some investigators discovered that Cxcl1 activates the Mac-1/ICAM-1 pathway promoting adhesion between leukocytes and endothelial cells.[39] Apart from promoting cell recruitment, CXCL1 induces $Ca^{2+}$-
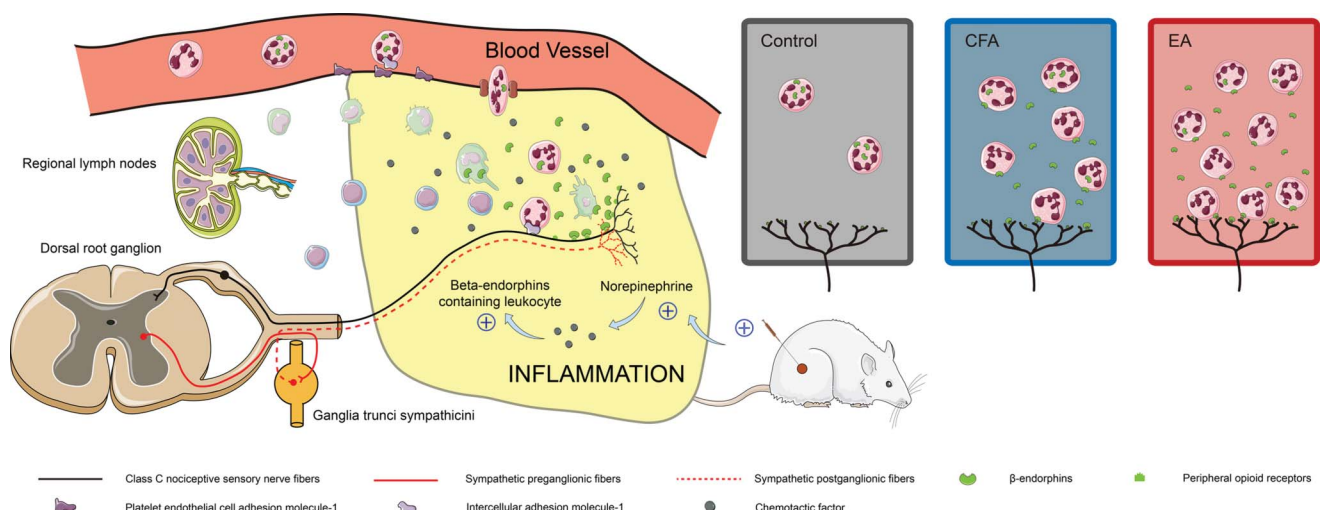


**Figure 6.** EA exerts a local analgesic effect during peripheral inflammation by activating sympathetic nerve fibers and promoting the migration of β-END containing immune cells to the pain site. β-END, β-endorphins; CFA, complete Frester adjuvant; EA, electroacupuncture.

regulated opioid release by activating the chemokine receptor CXCR2 on neutrophils and thereby inhibiting inflammatory pain.[29] Ccl5 exhibits a strong chemotactic activity toward T lymphocytes, monocytes, and macrophages expressing CCR5 receptor.[23,31] Because the results reported here demonstrate that EA treatment upregulated the transcription of *Cxcl1* and *Cxcl6*, we hypothesized that neutrophils are the primary type of opioid-containing leukocytes recruited to inflammatory sites (**Fig. 6**). Although the downregulation of *Ccl5* gene expression was observed, its role in EA-induced opioid-obtaining immune cells emigration is unknown.

Apart from acupuncture, other forms of traditional Chinese medicine techniques, including cupping and scraping act on the local site to treat pain diseases. These techniques are used clinically and have a comparable analgesic effect. Cupping and scraping therapy has the potential to cause subcutaneous bleeding points and produce local inflammatory reactions (blood cells leaving the circulation system can also chemotaxis and recruit immune cells). Based on the findings of this study and the conclusions, it is reasonable to infer that similar conventional medical therapies may exert a therapeutic effect on local pain by the peripheral analgesic effect of the immune system. Nonetheless, this mechanism remains to be demonstrated experimentally.

## 5. Conclusion

Taken together, our findings demonstrate that EA exerts peripheral analgesic effects at the site of inflammation by increasing the number of endogenous opiopeptides produced by peripheral immune cells in the local tissue. In addition, EA activates the sympathetic nerves, which recruits β-END–containing ICAM-1$^+$/CD11b$^+$ immune cells to the site of inflammatory pain and releases opiopeptides. The modulation of chemokines by local sympathetic activation is required for peripheral opioid peptide–mediated antinociception.

## Conflict of interest statement

The authors have no conflict of interest to declare.

## Acknowledgements

## Appendix A. Supplemental digital content

Supplemental digital content associated with this article can be found online at http://links.lww.com/PAIN/B798.

## References

[1] Akerman S, Kaube H, Goadsby PJ. Vanilloid type 1 receptors (VR1) on trigeminal sensory nerve fibres play a minor role in neurogenic dural vasodilatation, and are involved in capsaicin-induced dural dilation. Br J Pharmacol 2003;140:718–24.

[2] Binder W, Mousa SA, Sitte N, Kaiser M, Stein C, Schäfer M. Sympathetic activation triggers endogenous opioid release and analgesia within peripheral inflamed tissue. Eur J Neurosci 2004;20:92–100.

[3] Bing Z, Villanueva L, Le Bars D. Acupuncture and diffuse noxious inhibitory controls: naloxone-reversible depression of activities of trigeminal convergent neurons. Neuroscience 1990;37:809–18.

[4] Brack A, Labuz D, Schiltz A, Rittner HL, Machelska H, Schafer M, Reszka R, Stein C. Tissue monocytes/macrophages in inflammation: hyperalgesia versus opioid-mediated peripheral antinociception. Anesthesiology 2004;101:204–11.

[5] Cabot PJ, Carter L, Schafer M, Stein C. Methionine-enkephalin-and Dynorphin A-release from immune cells and control of inflammatory pain. PAIN 2001;93:207–12.

[6] Diamond MS, Staunton DE, de Fougerolles AR, Stacker SA, Garcia-Aguilar J, Hibbs ML, Springer TA. ICAM-1 (CD54): a counter-receptor for Mac-1 (CD11b/CD18). J Cell Biol 1990;111:3129–39.

[7] Duanmu CL, Wang XY, Zhang XN, He W, Su YS, Wan HY, Hu L, Wang Y, Jing XH. Electroacupuncture and transcutaneous electrical acupoint stimulation with different intensities relieve muscular of inflammatory pain of the rats [in Chinese]. Zhen Ci Yan Jiu 2020;45:902–7.

[8] Grisanti LA, de Lucia C, Thomas TP, Stark A, Strony JT, Myers VD, Beretta R, Yu D, Sardu C, Marfella R, Gao E, Houser SR, Koch WJ, Hamad EA, Tilley DG. Prior β-blocker treatment decreases leukocyte responsiveness to injury. JCI Insight 2019;5:e99485.

[9] Han JS. Acupuncture: neuropeptide release produced by electrical stimulation of different frequencies. Trends Neurosci 2003;26:17–22.

[10] Hua S, Cabot PJ. Mechanisms of peripheral immune-cell-mediated analgesia in inflammation: clinical and therapeutic implications. Trends Pharmacol Sci 2010;31:427–33.

[11] Kohm AP, Sanders VM. Norepinephrine and beta 2-adrenergic receptor stimulation regulate CD4+ T and B lymphocyte function in vitro and in vivo. Pharmacol Rev 2001;53:487–525.

[12] Kolaczkowska E, Kubes P. Neutrophil recruitment and function in health and inflammation. Nat Rev Immunol 2013;13:159–75.

[13] Kubota T, Mori H, Morisawa T, Hanyu K, Watanabe M, Tanaka TH. Influence of electroacupuncture stimulation on skin temperature, skin blood flow, muscle blood volume and pupil diameter. Acupunct Med 2020;38:86–92.

[14] Ley K, Laudanna C, Cybulsky MI, Nourshargh S. Getting to the site of inflammation: the leukocyte adhesion cascade updated. Nat Rev Immunol 2007;7:678–89.

[15] Liu J, Fu W, Yi W, Xu Z, Liao Y, Li X, Chen J, Liu X, Xu N. Extrasegmental analgesia of heterotopic acupuncture stimulation on visceral pain rats. Brain Res 2011;1373:160–71.

[16] Lorton D, Bellinger DL. Molecular mechanisms underlying β-adrenergic receptor-mediated cross-talk between sympathetic neurons and immune cells. Int J Mol Sci 2015;16:5635–65.

[17] Ma SX. Nitric oxide signaling molecules in acupoints: toward mechanisms of acupuncture. Chin J Integr Med 2017;23:812–5.

[18] Machelska H, Brack A, Mousa SA, Schopohl JK, Rittner HL, Schafer M, Stein C. Selectins and integrins but not platelet-endothelial cell adhesion molecule-1 regulate opioid inhibition of inflammatory pain. Br J Pharmacol 2004;142:772–80.

[19] Machelska H, Mousa SA, Brack A, Schopohl JK, Rittner HL, Schafer M, Stein C. Opioid control of inflammatory pain regulated by intercellular adhesion molecule-1. J Neurosci 2002;22:5588–96.

[20] Machelska H, Schopohl JK, Mousa SA, Labuz D, Schafer M, Stein C. Different mechanisms of intrinsic pain inhibition in early and late inflammation. J Neuroimmunol 2003;141:30–9.

[21] Medhurst SJ, Walker K, Bowes M, Kidd BL, Glatt M, Muller M, Hattenberger M, Vaxelaire J, O'Reilly T, Wotherspoon G, Winter J, Green J, Urban L. A rat model of bone cancer pain. PAIN 2002;96:129–40.

[22] Mousa SA, Shaqura M, Brendl U, Al-Khrasani M, Fürst S, Schafer M. Involvement of the peripheral sensory and sympathetic nervous system in the vascular endothelial expression of ICAM-1 and the recruitment of opioid-containing immune cells to inhibit inflammatory pain. Brain Behav Immun 2010;24:1310–23.

[23] Murooka TT, Rahbar R, Platanias LC, Fish EN. CCL5-mediated T-cell chemotaxis involves the initiation of mRNA translation through mTOR/4E-BP1. Blood 2008;111:4892–901.

[24] Nagashima H, Mahlakõiv T, Shih HY, Davis FP, Meylan F, Huang Y, Harrison OJ, Yao C, Mikami Y, Urban JF Jr, Caron KM, Belkaid Y, Kanno Y, Artis D, O'Shea JJ. Neuropeptide CGRP limits group 2 innate lymphoid cell responses and constrains type 2 inflammation. Immunity 2019;51: 682–95.e6.

[25] Nakai A, Hayano Y, Furuta F, Noda M, Suzuki K. Control of lymphocyte egress from lymph nodes through β2-adrenergic receptors. J Exp Med 2014;211:2583–98.

[26] Pinho-Ribeiro FA, Verri WA Jr, Chiu IM. Nociceptor sensory neuron-immune interactions in pain and inflammation. Trends Immunol 2017;38:5–19.

[27] Piqueras B, Connolly J, Freitas H, Palucka AK, Banchereau J. Upon viral exposure, myeloid and plasmacytoid dendritic cells produce 3 waves of distinct chemokines to recruit immune effectors. Blood 2006;107:2613–8.

[28] Rittner HL, Brack A, Machelska H, Mousa SA, Bauer M, Schafer M, Stein C. Opioid peptide-expressing leukocytes: identification, recruitment, and simultaneously increasing inhibition of inflammatory pain. Anesthesiology 2001;95:500–8.

[29] Rittner HL, Labuz D, Schaefer M, Mousa SA, Schulz S, Schafer M, Stein C, Brack A. Pain control by CXCR2 ligands through Ca²⁺-regulated release of opioid peptides from polymorphonuclear cells. FASEB J 2006;20:2627–9.

[30] Rittner HL, Mousa SA, Labuz D, Beschmann K, Schafer M, Stein C, Brack A. Selective local PMN recruitment by CXCL1 or CXCL2/3 injection does not cause inflammatory pain. J Leukoc Biol 2006;79:1022–32.

[31] Rossi D, Zlotnik A. The biology of chemokines and their receptors. Annu Rev Immunol 2000;18:217–42.

[32] Sanders VM, Straub RH. Norepinephrine, the beta-adrenergic receptor, and immunity. Brain Behav Immun 2002;16:290–332.

[33] Scheiermann C, Kunisaki Y, Lucas D, Chow A, Jang JE, Zhang D, Hashimoto D, Merad M, Frenette PS. Adrenergic nerves govern circadian leukocyte recruitment to tissues. Immunity 2012;37:290–301.

[34] Sharma D, Farrar JD. Adrenergic regulation of immune cell function and inflammation. Semin Immunopathol 2020;42:709–17.

[35] Stein C, Hassan AH, Przewłocki R, Gramsch C, Peter K, Herz A. Opioids from immunocytes interact with receptors on sensory nerves to inhibit nociception in inflammation. Proc Natl Acad Sci 1990;87:5935–9.

[36] Szabo I, Chen XH, Xin L, Adler MW, Howard OMZ, Oppenheim JJ, Rogers TJ. Heterologous desensitization of opioid receptors by chemokines inhibits chemotaxis and enhances the perception of pain. Proc Natl Acad Sci 2002;99:10276–81.

[37] Trier AM, Kim BS. Sensory neurons drive anticipatory immunity. Cell 2019;178:771–3.

[38] Vickers AJ, Vertosick EA, Lewith G, MacPherson H, Foster NE, Sherman KJ, Irnich D, Witt CM, Linde K. Acupuncture for chronic pain: update of an individual patient data meta-analysis. J Pain 2018;19:455–74.

[39] Wang H, Hong LJ, Huang JY, Jiang Q, Tao RR, Tan C, Lu NN, Wang CK, Ahmed MM, Lu YM, Liu ZR, Shi WX, Lai EY, Wilcox CS, Han F. P2RX7 sensitizes Mac-1/ICAM-1-dependent leukocyte-endothelial adhesion and promotes neurovascular injury during septic encephalopathy. Cell Res 2015;25:674–90.

[40] Wang Y, Gehringer R, Mousa SA, Hackel D, Brack A, Rittner HL. CXCL10 controls inflammatory pain via opioid peptide-containing macrophages in electroacupuncture. PLoS One 2014;9:e94696.

[41] Xu J, Gao XP, Ramchandran R, Zhao YY, Vogel SM, Malik AB. Nonmuscle myosin light-chain kinase mediates neutrophil transmigration in sepsis-induced lung inflammation by activating β2 integrins. Nat Immunol 2008;9:880–6.

[42] Young EA, Houghten RA, Akil H. Degradation of [3H]β-endorphin in rat plasma is increased with chronic stress. Eur J Pharmacol 1989;167:229–36.

[43] Zhao ZQ. Neural mechanism underlying acupuncture analgesia. Prog Neurobiol 2008;85:355–75.

[44] Zhu B, Xu WD, Rong PJ, Ben H, Gao XY. A C-fiber reflex inhibition induced by electroacupuncture with different intensities applied at homotopic and heterotopic acupoints in rats selectively destructive effects on myelinated and unmyelinated afferent fibers. Brain Res 2004; 1011:228–37.